Kinetic constraints on illitization reactions and the effects of organic diagenesis in sandstone/shale sequences

Gilles Berger*

URA 67 CNRS, Université Paul-Sabatier, 38 rue des Trente-six-Ponts, 31400 Toulouse, France

Jean-Claude Lacharpagne

Elf Aquitaine Production, CSTJF, Avenue Larribau, 64018 Pau, France

Bruce Velde

URA 1316 CNRS, Ecole Normale Supérieure, 24 rue Lhomond, 75005 Paris, France

Daniel Beaufort

URA 697 CNRS, Université de Poitiers, 40 Av. du Recteur Pineau, 86022 Poitiers, France

and

Bruno Lanson

LGIT-IRIGM, URA 733 CNRS, BO 53 X, 38041 Grenoble Cedex, France

Abstract—Based on water–rock interaction modelling and kinetic considerations, the present study is aimed at testing the impact of organic matter maturation on two kinds of diagenetic reactions leading to the alteration of the petrophysical properties of sandstones: (1) Clay mineral conversion to illite with K-feldspar being a local potential source of K; and (2) Dissolution–precipitation processes produced in sandstones by the action of water-soluble organic species derived from adjacent shales.

Assuming firstly that the chemical reactions take place in closed systems, the nature and timing of diagenetic reactions in marine sandstone/shale formations were modelled for a 50–120°C temperature range in order to improve understanding of the factors that control the illitization reaction with K-feldspar co-existing with aluminous clay. Illite is modelled here as a muscovite type mineral. We tested the effects of an energy barrier on illite growth by allowing or preventing the muscovite/illite precipitation reaction to occur, while using several illitization reaction rates. We also compared the stable mineral parageneses predicted for organic material-free systems with those predicted in the case of organic diagenesis (release of CO_2, CH_4, acetic and oxalic acids). Similarities and discrepancies between numerical results and natural mineral assemblages suggest that the illitization reaction depends on the nature of the reacting clays. Kaolinite conversion to end-member illite involves high-energy conditions (> 2 kcal mol^{-1}), which are not met when the pore water equilibrates with the mineral matrix from undersaturated conditions in a closed system. To overcome this barrier, the fluid should be oversaturated with respect to K-feldspar. An external source of K or a pH increase in an open system is necessary for this reaction. No particular effect of organic diagenesis on this reaction was found in the present study. On the other hand, smectite-to-illite conversion involves a lower energy barrier and can operate in closed systems where K-feldspars are the source of K. The maturation of organic matter may speed up the smectite-to-illite conversion rate by increasing the Gibbs Free Energy of illite growth.

Interactions between sandstone and shale were examined by modelling the transfer of aqueous species of organic origin from shale to sandstone. Fluid expulsion from shale had little or no effect on diagenesis in adjacent sandstones during each flushing cycle, mainly because organic protons and ligands were neutralized in the source rock. However, the diffusion of shale-derived cations through sandstone as organometallic complexes (Mg > Ca > > Fe > > Al) appears to be an efficient process during carbonate cementation in sandstones, where oxidizing conditions enhance the decomposition of such complexes. © 1997 Elsevier Science Ltd. All rights reserved

INTRODUCTION

The chemical reactions affecting the rock-forming minerals in sedimentary basins are, together with compaction, the main causes of porosity and permeability changes in the rocks. Increasing temperature and pressure with depth, added to fluid flow through the sediments, has led to chemical disequilibria between the aqueous phase and the mineral matrix. In response to these disequilibria, dissolution and precipitation reactions have maintained the water-rock system close to chemical equilibrium. Petrographic data generally provide evidence of these

---

* Laboratoire Géochimie, 38 rue des 36 Ponts, 31400 Toulouse, France, tel: (33) 61 55 62 40 fax: (33) 61 52 05 44, email: berger@lucid.ups-tlse.fr.

reactions. However, thermodynamic and kinetic conditions are often useful in unravelling complex geological histories.

Most of the mineralogical reactions observed in clastic sediments are practically isochemical with the sources and sinks of elements occurring in the vicinity of reaction sites. Biotite chloritization and quartz overgrowths produced by pressure solution, as well as illitization of aluminous clays caused by concomitant dissolution of K-feldspar, are all typical of this kind of reaction. On a mm or cm scale, these reactions can be modelled for a closed system as a function of time, temperature or initial mineral assemblage, provided that the kinetic laws governing the reaction are well known. For most silicates and carbonates, the dissolution rates and relations of these rates to temperature, pH, fluid chemistry and chemical affinity are well documented. However, much less is known about the kinetics of nucleation and growth of authigenic silicates during burial. As an example, Ehrenberg (1991), Bjørlykke and Aagaard (1992) and Ehrenberg *et al.* (1993) have reported the occurrence of residual kaolinite or dickite and K-feldspar in North Sea sandstones at 3000–4000 m depths. This is in contradiction with the existing thermodynamic conditions in the boreholes, which indicate that the reaction K-feldspar + kaolinite → illite + quartz should have taken place at a much lower temperature leading to the disappearance of either kaolinite or K-feldspar. On the other hand, the observed kaolinite illitization occurred within a restricted space of time (Platt, 1993; Matthews *et al.*, 1994; Lanson *et al.*, 1996). In contrast, the conversion of smectite to illite observed in shales is described as a slow but systematic reaction (Velde and Vasseur, 1992). This duality in clay diagenesis raises questions about the factors controlling illitization.

On a larger scale, juxtaposed geological formations of different compositions can also produce diagenetic reactions either by diffusion of aqueous species or by displacement of the whole fluid phase through the sediment. In sandstone/shale sequences, for example, dissolution of feldspar and precipitation of aluminous clays in sandstones are interpreted as resulting from the release of acid organic species from adjacent organic material-rich shales or coals (Ehrenberg, 1991; Gaupp *et al.*, 1993; Platt, 1993). However, under such conditions, the capacity of a moving fluid to produce diagenetic reactions is difficult to quantify from petrographic data alone. Numerical simulation of water–rock interactions appears here as a useful tool in constraining the geochemical diagenetic patterns in sedimentary basins.

In this study, we use thermo-kinetic modelling of extreme cases in order to test several diagenetic reaction pathways in sandstone/shale sequences. We focus on two kinds of mineral reactions: (1) Clay mineral conversion to illite with K-feldspar being a local potential source of K; and (2) Dissolution–precipitation processes produced in sandstones by the action of water-soluble organic species generated in the sandstone itself, or derived from adjacent shales. In the latter case, the effects of the transfer of water-soluble organic species (carbonates and acetates) are modelled from source shales to adjacent sandstones using advection or diffusion as the transfer mechanism. From similarities and discrepancies between the numerical results and field data, we first identify the mechanism that controls the illitization reaction observed in clastic sediments, and then we discuss the effect of organic matter maturation on diagenesis in sandstone/shale sequences.

REACTION PATHWAY AND KINETIC CONSTRAINTS USED FOR SIMULATIONS

The nature and timing of diagenetic reactions in a marine sandstone/shale sequence were calculated using the EQ3/6 software package (Wolery, 1983; Wolery and Daveler, 1990). Briefly, 3 kinds of quantitative information can be generated:

(1) The chemical force which drives a given reaction (Gibbs Free Energy of reaction);
(2) The nature of the stable paragenesis as a function of the temperature and initial sediment composition;
(3) The time required to reach thermodynamic equilibrium as a function of the specified kinetic laws.

A first set of calculations was performed for a clean sandstone, an argillaceous sandstone and a shale containing organic material, assuming dissolution and precipitation reactions in a closed system at temperatures of 50, 80 and 120°C. This thermal window reveals the diagenetic events occurring in sedimentary deposits to a depth of about 4000 m, assuming a mean geothermal gradient of 27°C/km and a surface temperature of 12°C. In the case of sandstones, we compared the timing of reactions and the stable mineral paragenesis predicted for organic-free systems with the values predicted for water-soluble organic species generated within sandstones. We also modelled the fluid expelled from a shale containing organic material towards to an organic-free argillaceous sandstone, and the thermal decomposition of acetate species at 120°C. The general reaction pathway is shown in Fig. 1.

Starting fluid

The starting fluid is seawater. We used both standard and 'reduced' seawater (pH$_{(25°C)}$ = 4.2 and Eh$_{(25°C)}$ = − 250 mV), assuming SO$_4$ bacterial reduction during early diagenesis. Because of the low water–rock ratios in closed systems (W/R < 0.1), no significant difference was observed in the final paragenesis. The activity coefficients of water and aqueous
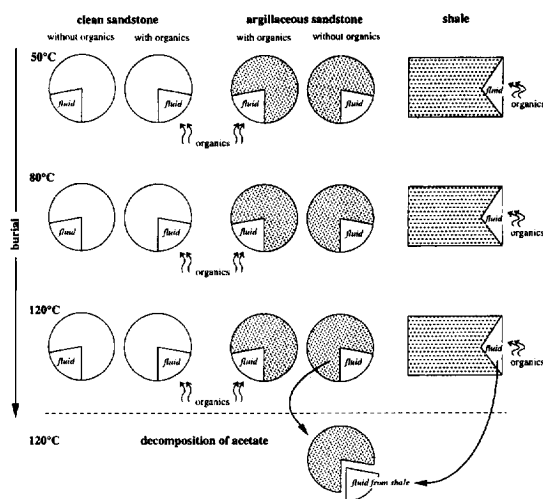
Fig. 1. Reaction pathways in closed system simulations. At each temperature, the starting mineralogy is reacted with the starting fluid.

species were calculated using B-equations (Helgeson, 1969).

Starting mineral paragenesis:

Three mineral matrices were tested that correspond to the main sedimentary lithologies observed in sandstone/shale sequences:

(1) Mature sandstone containing 66% quartz, 6% muscovite and 6% microcline (by volume) and having 22% porosity;

(2) Argillaceous sandstone made up of 60% quartz, 6% muscovite, 6% microcline and 6% Al-clays (by volume), with 22% porosity. the Al-clays consist of kaolinite, Mg-beideillite or Mg-montmorillonite ('Mg-' means saturated with Mg). Note the increased Mg/Al ratios in the clay fraction;

(3) Shale or silt, containing equal volumes of quartz, microcline, muscovite, and Al–Mg–Fe–Ca–clays (Ca-beidellite + Mg-nontronite). The porosity of shale was estimated at 10%, assuming that the compaction of these sediments occurred at a temperature of less than 50°C ($\approx$ 1700 m).

Organic diagenesis

The main water-soluble species generated during the thermal breakdown of kerogen are CO_2, organic acids and CH_4. According to Barth (1991) and other authors, acetate is the most abundant organic anion in natural waters. Carbon dioxide has several possible origins: thermal breakdown of kerogen or decarboxylation of organic acids (Kharaka et al., 1983, 1985; Drummond and Palmer, 1986; Bell et al., 1994). The relative amounts of CO_2, organic acids, and CH_4

generated from the thermal breakdown of kerogen can be estimated from hydrous pyrolysis as a function of the nature of the source rock and kerogen maturity (Barth and Bjørlykke, 1993; Andresen et al., 1994). In the present study, the progressive breakdown of kerogen (50 mg per gram solution) is modelled by dissolving increasing amounts of CO_2 and acetic acid in the aqueous phase at increasing temperatures. The cumulative amounts of released organic species are selected from the above-mentioned studies, using the maximum concentration of organic acids found in oil-field water (10 000 ppm; MacGowan and Surdam, 1988). We also modelled the thermal decomposition of acetic acid into CH_4 and H_2CO_3 acid at 120°C. The association constants of Al, Fe, Mg and Ca acetate complexes reported by Harrison and Thyne (1992) are incorporated into the database to allow for the existing organometallic complexes. In order to determine the reaction rate of the mineral matrix alone, the organic species are added to the aqueous phase—at the beginning of reaction—in amounts varying with temperature, as shown in Table 1.

Dissolution rate of the mineral matrix

The rate of a chemical reaction at the solid-solution interface depends on the surface area of the interface, the reaction rate constant and the fluid chemistry. These parameters are constrained for the dissolution reactions as follows:

(1) The selected grain size of sediments is taken arbitrarily as 200 μm for sandstones and 20 μm for shales. The interfacial area between the sediment and pore fluid (i.e. the specific surface area of the fluid) is determined using the equation for close-packed spheres reported by Rimstidt and Barnes (1980). These areas are 42.75 m^2 l^{-1} for sandstones and 427.5 m^2 l^{-1} for shales. The macroscopic surface area assigned to each mineral exposed to pore water is assumed to be proportional to the mineral volume in the rock. We also took into account the fact that the surface area decreases as the mineral dissolves. Since feldspathic minerals usually exhibit etch pits, fractures and cleavages at their surfaces, the specific surface area of microcline is estimated to be 10 times greater than its macroscopic surface (White and Peterson, 1990). For clays, a crystallite size of 200 μm, or even

Table 1. Cumulative amounts of organic species supplied to the aqueous phase

Temperature	CO_2	CH_3COOH (mole kg^{-1})	CH_4	total mass (g kg^{-1})
50°C	0.125	0.05	0.0	8.5
80°C	0.5	0.15	0.0	31.0
120°C	0.85	0.15	0.0	46.4
120°C*	1.0	0.0	0.15	

*(decarboxylation of acetate)

20 μm, appears to be a significant overestimation. Their specific surface area is estimated to be 100 times larger than the macroscopic surface area calculated as above, thus corresponding to sheets of thickness 2.0 and 0.2 μm in sandstones and shales, respectively. No geometric correction was made either for quartz or for muscovite, according to Nonaka (1984).

(2) The dissolution rate constants for quartz at 50, 80 and 120°C are calculated from the rate-temperature dependence in pure water, as reported by Dove and Crerar (1990). For microcline and muscovite, the rate constants at low temperatures reported by Busenberg and Clemency (1976) and Lin and Clemency (1981) are extrapolated using an activation energy of 40 kJ mole^{-1}, which characterizes the dissolution rate of most of the silicates under near-neutral pH conditions (Helgeson *et al.*, 1984). In the case of clay minerals, for which the hydrolysis rates are poorly documented, the rate constants and activation energies are used for neutral pH values as reported for kaolinite by Carroll and Walther (1990). We disregarded the pH dependence because preliminary tests show that pore waters are buffered by the mineral assemblage under near-neutral pH conditions.

(3) According to the transition state theory, the dissolution or precipitation rate of silicates is also a function of the degree of solution saturation, or equivalently the Gibbs Free Energy of reaction. Rimstidt and Barnes (1980) and Berger *et al.* (1994) have shown that the dissolution rate of quartz in near-equilibrium conditions obeys a first-order affinity relation. Nagy *et al.* (1991) reported a similar behaviour for the dissolution of kaolinite. In contrast, Burch *et al.* (1993) and Oelkers *et al.* (1994) found that a single-rate relation controlled by solution saturation does not accurately describe the aluminosilicate dissolution rates over the complete range of chemical affinity. However, the data reported by these last authors were obtained in acidic or basic conditions, i.e., in conditions where charged surface species promote the far-from-equilibrium dissolution rates. In the absence of more constrained kinetic models, using conditions close to equilibrium in the 5–8 pH

range characterizing the natural waters, the dissolution rates of the starting phases were all described using a first-order affinity relation and assuming a stoichiometric release of chemical constituents.

The dissolution rate constants and the surface area for the starting mineral phases are shown in Table 2. Note that shale and sandstone are not only defined by their grain size (by an appropriate choice of specific surface areas), but also by their different mineralogical compositions.

Precipitation rate of secondary phases

Several assumptions are made for the precipitation rates of secondary phases:

(1) No specific precipitation rate is selected for a first set of calculations. The stable secondary phases are precipitated at each step of the reaction in the amounts required to maintain the pore water in equilibrium with these phases. Illite is modelled on secondary muscovite, according to the composition of end-member illite reported by Lanson and Champion (1991). For this case, the precipitation rates of secondary phases are assumed to be much higher than the dissolution rates of source minerals. Thus, the amounts of precipitated secondary phases are controlled by the hydrolysis rate of the starting mineral matrix.

(2) Even if the above assumption is valid for the precipitation of oxides, hydroxides and carbonates during silicate alteration, it seems questionable in the case of illite growth (see Introduction). To allow for the commonly observed preservation of kaolinite at high temperatures in K-feldspar-bearing sandstones, the secondary parageneses in mature and argillaceous sandstones is also calculated by impeding the precipitation reaction of muscovite/illite. The degree of supersaturation of the pore fluid is thus calculated with respect to muscovite/illite, or the Gibbs Free Energy of illite growth, when the fluid is in equilibrium with the starting mineral matrix, in particular with Al-clays and K-feldspar. The absence of muscovite/illite

Table 2. Input constraints for the starting mineral phases

Temperature	Quartz	Muscovite	Microcline	Al, Mg-clays (kaol. Beid. mont.)	Fe,Mg-clays (nont.)
			rate (mole m^{-2} s^{-1})		
50°C	7.4 10^{-12}	3.9 10^{-13}	2.1 10^{-12}	4.7 10^{-14}	4.7 10^{-14}
80°C	3.8 10^{-11}	1.3 10^{-12}	7.1 10^{-12}	7.9 10^{-14}	7.9 10^{-14}
120°C	5.0 10^{-10}	5.0 10^{-12}	2.7 10^{-11}	1.0 10^{-13}	1.0 10^{-13}
			Lithology surface area (m^2 kg^{-1})		
Mature sand.	28.2	2.56	25.6	/	/
Argil. sand.	25.6	2.56	25.6	256	/
Shale	96.5	96.5	965	4809	4809
			mineral/solution ratio (moles kg^{-1})		
Mature sand.	132	2.0	2.5	/	/
Argil. sand.	120	2.0	2.5	2.5 or 2.7	/
Shale	100	16.5	20.6	8.3	8.3

precipitation in shales is not tested here because the illitization reaction occurred systematically.

(3) Finally, for the kaolinite-bearing sandstones, the illitization reaction is constrained by the precipitation rate of muscovite/illite rather than by the dissolution rate of source minerals. Chermack and Rimstidt (1990) have determined experimentally the kaolinite-to-illite conversion rate in the presence of muscovite as a function of temperature (250–307°C), surface area of muscovite, pH and the concentration of K in solution. We use the rate value and the activation energy proposed by Chermack and Rimstidt (1990), assuming that the K^+/H^+ ratio in solution is given by the coexistence of microcline and kaolinite and that illite nucleates at the surface of muscovite as observed by these authors.

TIMING AND MINERALOGICAL CHANGES DURING SIMULATIONS

Four parameters are systematically tested from simulations: temperature, organic diagenesis in sandstones, nature of clays in argillaceous sandstones, and the kinetics of muscovite/illite precipitation in sandstones. The effects of these parameters on the reaction timing and final paragenesis are described below for each type of rock.

Diagenesis in organic-bearing shales (no kinetic constraints on illite growth)

The solution very quickly approaches equilibrium with quartz and primary muscovite after dissolution of trivial amounts of these phases. The main mineral reaction involves dissolution of microcline and beidellite, with production of secondary muscovite/illite and quartz until complete disappearance of beidellite. The reaction is complete within less than 2000 a at 50°C, with decreased duration at higher temperatures. Minor reactions include the precipitation of traces of carbonate, anhydrite and zeolite, as well as the exchange of Mg with Ca in nontronite. Although acid species of organic origin are generated in the aqueous phase (CO_2, acetic acid), the solution is buffered at near-neutral pH at all temperatures. A more detailed description is given in the discussion on interactions between shales and sandstones.

Diagenesis in clean sandstones

Diagenesis in clean sandstones produces few mineralogical reactions. In the absence of organic diagenesis, the pore fluid equilibrates with the starting mineral assemblage under near-neutral pH conditions at all temperatures, with no significant change for solids. Upon addition of CO_2 and acetic acid to the aqueous fluid, a small fraction of initial microcline is

seen to dissolve (passing from 10% at 50°C to 16% at 120°C), producing secondary muscovite/illite and quartz, or kaolinite if the precipitation reaction of muscovite/illite is impeded. The time required to reach equilibrium never exceeds 500 years.

Diagenesis in argillaceous sandstones

The results obtained for argillaceous sandstones are more scattered given the number of parameters tested (temperature, nature of the starting clays, muscovite/illite precipitation reaction, with or without constraint, presence or absence of organic materials, illite growth rate relation, using the shale-derived fluid at 120°C).

When precipitation of muscovite/illite is unimpeded, microcline and initial clays, whatever their nature (kaolinite, beidellite or montmorillonite), dissolve into illite + quartz until complete disappearance of feldspars or other clays. The CO_2 and organic acid generated by organic diagenesis has no significant effect on the reaction pathway. The pH of the equilibrated pore water ranges in the 4.2–6.5 interval. The time required to reach equilibrium decreases as temperature increases, passing from 5100 a at 50°C to 360 a at 120°C.

If the precipitation of muscovite/illite is impeded, microcline does not dissolve and the behaviour of Al-clays is conditioned by the nature of the clay, temperature conditions, and organic diagenesis. The last factor can be viewed as a source of protons for mineral reactions. The secondary parageneses are shown in Fig. 2. Kaolinite is stable in all cases. Beidellite is converted to kaolinite, montmorillonite and quartz, depending on temperature as well as the amounts of CO_2 and acetic acid released into the
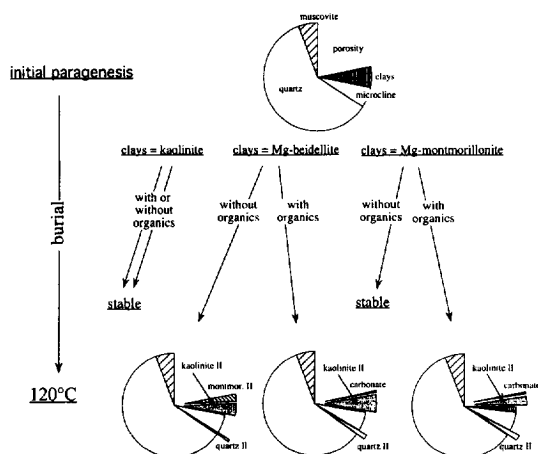

Fig. 2. Changes in the mineral paragenesis of argillaceous sandstones assuming no precipitation of muscovite/illite. Sectors are proportional to the volumetric mineral mode in the rock, while secondary phases are indicated with an expanded radial scale.

aqueous phase. Montmorillonite remains stable in organic matter-free systems, but is partially converted to kaolinite + quartz upon release of protons of organic origin into the pore water. It is noteworthy that the initial Al-clays are the precursors of authigenic kaolinite and that K-feldspar remains stable. In all cases, the time necessary to reach equilibrium does not exceed 150 a. The Gibbs Free Energy of the impeded muscovite/illite precipitation (i.e. the chemical potential which should drive the impeded reaction) is plotted against temperature and starting clays in Fig. 3 (the higher the absolute value of the Gibbs Free Energy, the higher the chemical potential for precipitation of illite). Using montmorillonite as the starting clay, and in the absence of organic diagenesis, the $|\Delta G|_{reaction}$ for illite growth decreases with temperature from 1.4 kcal mole^{-1} at 50°C to 1.18 kcal mole^{-1} at 120°C. In all other cases, illite oversaturation is controlled at the end of the reaction by the same mineral assemblage (microcline–quartz–kaolinite), and the $|\Delta G|_{reaction}$ for illite growth increases from 1.4 kcal mole^{-1} at 50°C to 1.96 kcal mole^{-1} at 120°C.

When the precipitation of muscovite/illite is constrained by the rate value proposed by Chermack and Rimstidt (1990), the reaction is completed after 4.5 Ma at 50°C, 0.015 Ma at 80°C and 417 a at 120°C.

When reacting the organic material-free argillaceous sandstones with the shale-derived fluid at 120°C (Fig. 1), results are similar to those obtained when using unreacted seawater with the only difference that traces of carbonate precipitate after decomposition of the acetate species contained in the shale-derived fluid.

KINETIC CONTROL OF ILLITE GROWTH

As appears from the above calculations, the theoretical time required for the system to reach chemical equilibrium is very short if it is dependent on dissolution reactions alone (no kinetic constraints on the precipitation reactions). The longest elapsed time (5100 a in argillaceous sandstones) is obtained upon dissolution of microcline and Al-clays into illite + quartz at 50°C. It is clear that these calculated times are underestimated by several orders of magnitude. In particular, they suggest that K-feldspar dissolution in the presence of Al-clays must have been complete at the time of early diagenesis, unlike the situation generally observed in sandstones (Ehrenberg, 1991; Bjørlykke and Aagaard, 1992; Ehrenberg *et al.*, 1993). According to Bjørkum and Gjelsvik (1988), the coexistence of K-feldspar and kaolinite in North Sea sandstones may indicate pore water supersaturation with respect to quartz at low temperatures. But according to Kharaka *et al.* (1985) and Egeberg and Aagaard (1989), the silica contained in pore water is in equilibrium with quartz at temperatures higher than 70°C. Consequently, the occurrence of kaolinite in

deep K-feldspar-bearing sandstones raises a question as to the true factors controlling illitization and the validity of the kinetic constraints used in our calculations. Four assumptions are problematic:

Illite composition. In this study, we use a mica (muscovite) to model end-member illite. This assumption is based on the mica-type composition of the latter, as reported in Srodon *et al.* (1986) and Lanson and Champion (1991). However, natural end-member illite contains some smectitic sheets due to restricted substitution of Al by divalent cations (mainly Mg). Considering the end-member illite as a true Mg phase, the availability of Mg could then become the limiting factor of kaolinite-to-illite conversion as modelled in Ben Baccar *et al.* (1993). This explanation is rejected here because: (1) The smectitic sheets in end-member illite can be viewed as defects; (2) Natural shales or sandstones always contain Mg; and (3) Chermack and Rimstidt (1990) transformed kaolinite into illite in Mg-free experimental systems.

Dissolution rates as constraints. Based on our calculations, the rate-limiting reaction is the dissolution of microcline when the illitization rate is constrained by the dissolution of source minerals. We established that any change in the kinetic parameters of microcline leads to an equivalent change in the calculated reaction time and that the kinetic parameters of clays are of secondary importance, due to the high specific surface area used for clays. The parameters determining the reaction rate of microcline are the surface area, the rate constant, the order of the affinity relation, and solution chemistry. Assuming that all these parameters are overestimated, we calculate the rate of the reaction, microcline + kaolinite → quartz + muscovite/illite by decreasing the surface area and rate constant of microcline by one order of magnitude, and by controlling the concentration of silica in solution using chalcedony instead of quartz. The recalculated time values required to reach equilibrium in sandstone are 0.486 Ma, 0.180 Ma and 0.045 Ma at 50, 80 and 120°C, respectively. Although these new constraints result in a 120- to 150-fold reduction of the reaction rate, they do not resolve the question of metastability of the kaolinite + K-feldspar assemblage in sandstones. This suggests that illite nucleation and growth are likely to be a limiting factor in illitization. Furthermore, the pore water equilibrates very rapidly with the mineral present in the rock, at least 'from the bottom' (undersaturated conditions).

Precipitation rate as a limiting step. Using the rate values proposed by Chermack and Rimstidt (1990) to constrain the precipitation of muscovite/illite, the illite growth reaction appears to be a limiting factor only at low temperature (4.5 Ma for the complete reaction at 50°C). However, it cannot be regarded as a limiting

factor for deeply buried sandstones on a geological time scale.

Nucleation as a kinetic barrier. Nucleation is the final process capable of limiting the rate of an illitization reaction. Calculations carried out in the case of an impeded muscovite precipitation reaction help determine the oversaturation of muscovite/illite in clastic sediments with pore water in equilibrium with microcline, clays and quartz. Figure 3 shows how the Gibbs Free Energy of the muscovite/illite precipitation reaction depends on the nature of the clays co-existing with K-feldspar. Using kaolinite, the $|\Delta G|_{reaction}$ for muscovite/illite precipitation increases with temperature, while it decreases (with temperature) in the presence of montmorillonite. This suggests that the activation barrier to illite growth (i.e. the minimum $|\Delta G|_{reaction}$ for the reaction to occur) is more easily overcome with burial in the presence of kaolinite rather than smectite. However, this assumption is in apparent contradiction with the fact that K-feldspar and kaolinite can survive illitization in sandstones at depths up to 4000 m (Ehrenberg, 1991; Bjørlykke and Aagaard, 1992; Ehrenberg et al., 1993), while, in shales, the conversion of smectite to illite is described as a slow but systematic reaction (Velde and Vasseur, 1992). This can be explained by the nature of the reaction. The illitization of smectite in a mixed-layer structure involves a progressive enrichment in end-member illite, while illitization of kaolinite involves precipitation of the pure end-member illite without any intermediate members of the series. Note that direct precipitation of end-member illite is also envisaged in the smectite-to-illite transformation, but as a late and very slow reaction (Lanson and Champion, 1991). In the first type of reaction, the

Fig. 4. Illitization process as a function of the nature of the initial clays.

activation barrier is likely to be lower than in the case of direct precipitation of a muscovite-type mineral. Thus, it appears that smectite is more suited as a precursor to illite than kaolinite. Based on these considerations, we propose two different reaction pathways to account for the illitization of sedimentary clays, depending on the nature of the clays rather than the lithology (shale or sandstone). These pathways are shown schematically in Fig. 4.

Kaolinite-to-illite conversion

Two reactions can account for this conversion:

K-feldspar + kaolinite → muscovite/illite
$+2$ quartz + H_2O (closed system)　　　(1)

kaolinite + $2/3K^+$ → $2/3$ muscovite/illite
$+2/3H^+$ + H_2O (open system)　　　(2)

The survival of K-feldspar and kaolinite—as observed in North Sea sandstones—demonstrates that the metastability of this assemblage can continue through geological time. Even a $|\Delta G|_{reaction}$ of 2 kcal mole^{-1}, calculated at 120°C, is insufficient to produce the direct precipitation of end-member illite in these sediments according to reaction (1). Thus, if kaolinite is illitized at a shallower depth, it can be said that increasing temperature is not the controlling factor. According to Rossel (1982), Pye and Krinsley (1986) and Lanson et al. (1996), the intense illitization
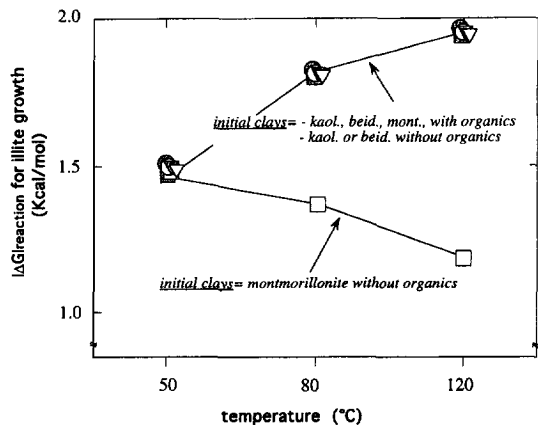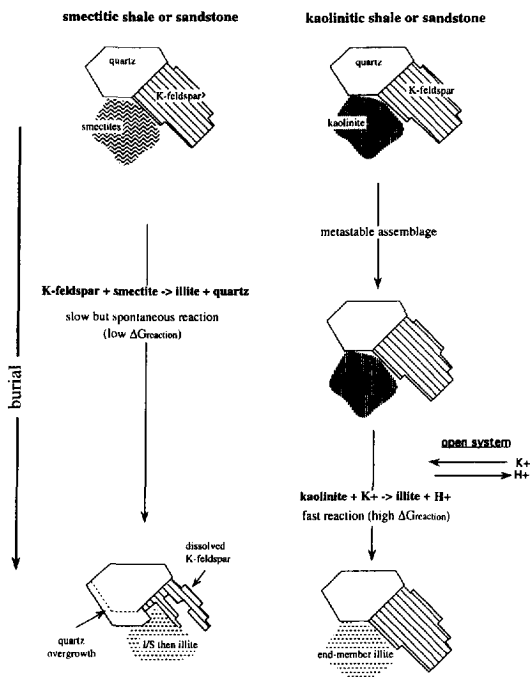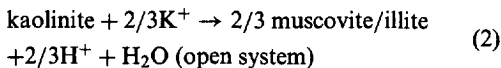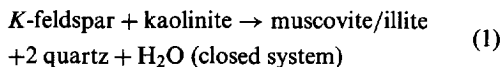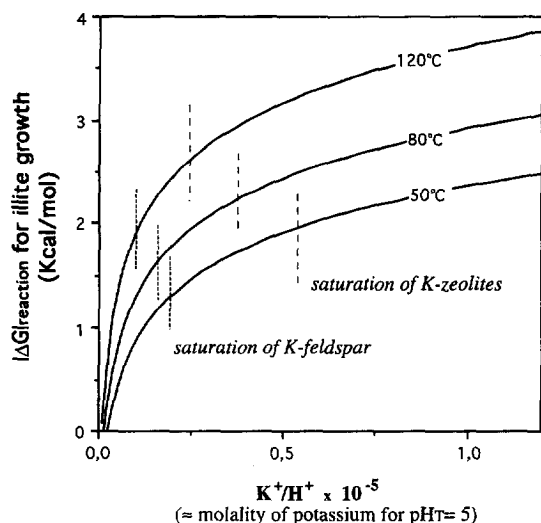

Fig. 3. Gibbs Free Energy for muscovite/illite precipitation, (when this reaction is ignored in calculations), plotted versus the temperature and nature of initial clays (triangles indicate kaolinite, circles beidellite, squares montmorillonite). The open symbols are for organic matter-free systems and closed symbols are for the organic matter-bearing systems.

Fig. 5. Increase in the scale of the $|\Delta G|_{reaction}$ for illite growth versus the K^+/H^+ activity ratio, when impeding the precipitation of all potassic phases. The vertical dashed lines show the stability limits of K-feldspar and K-zeolites.

of kaolinite in North Sea sandstones may be related to an invasion of sediments by brines. As a result, these saline solutions, which are enriched in K, increase the degree of saturation of all the K-bearing phases, including muscovite/illite and K-feldspar. We tested the hypothesis of water flushing by increasing the K^+/H^+ activity ratio in the pore water (increase of aqueous K or pH) and by assuming that SiO_2 and Al are buffered by quartz and kaolinite. Increase in the $|\Delta G|_{reaction}$ for illite growth (oversaturation of illite) is shown against the K^+/H^+ activity ratio in Fig. 5 with impeded precipitation of all potassic phases. Figure 5 suggests that if K-feldspar does not precipitate immediately when it becomes oversaturated, then the $|\Delta G|_{reaction}$ for illite growth can reach a critical value beyond which the reaction (2) will start. Under these conditions, K-feldspar is oversaturated and cannot be a source of K. This implies that an external source of K is necessary for kaolinite illitization. This also implies that the degree of illitization depends on the supply of K and equivalent consumption of protons (to avoid a decrease in the K^+/H^+ activity ratio). The buffering capacity of aqueous or mineral carbonates appears here to be an optimizing factor in kaolinite illitization. No effect of organic matter maturation on the kaolinite-to-illite conversion is indicated by the calculations. According to Small (1993), transportation of aluminum and potassium as oxalate complexes could also drive reaction (2) in an open system. However, the conditions for such a process are restricted and are discussed in the latter section.

Smectite-to-illite conversion

Velde and Vasseur (1992) derived a two-step kinetic model for smectite-to-illite conversion based

on the reactions observed in three sedimentary basins (U.S.A. and Japan). Although the behaviour of the K-feldspar contained in the samples taken from these basins is not studied, one can assume with Hower *et al.* (1976) and Eberl (1993) that feldspar hydrolysis is the source of potassium for the fastest step in the Velde and Vasseur's model (reaction $R_0 \rightarrow R_1$), as defined in the present study. This assumption is also supported by the experimental results reported in Hellmann (1994) and Berger (1995), which suggest that the activation energy of the dissolution of feldspar minerals (68.8 KJ mol^{-1} for albite at neutral pH) is much higher than that proposed by Helgeson *et al.* (1984) and close to that found by Velde and Vasseur (1992) for the $R_0 \rightarrow R_1$ reaction (69.7 KJ mol^{-1}). In this case, the similarity in the activation energy values could reflect the control of the dissolution step of feldspar on the overall $R_0 \rightarrow r_1$ reaction rate. However, Velde and Vasseur's model predicts complete conversion of smectite to illite at a much slower rate (several Ma, depending on temperature) than that calculated from the present simulations when the overall rate is controlled by dissolution of the primary minerals. These rate differences can be attributed to uncertainties in kinetic constraints (surface area of starting minerals, aqueous silica concentration at low temperatures, rate constants for clays, etc.), and also because the natural precipitation of illite proceeds in oversaturated conditions. Thus, the higher the oversaturation of illite, the slower the $|\delta G|_{reaction}$ for K-feldspar dissolution and the slower the illitization rate. The second and much slower step in Velde and Vasseur's model, which corresponds to the addition of an end-member illite to the i/s material, can be viewed as a transition from a first generation of illite (or detrital muscovite?) to another end-member illite. This reaction was not modelled here because we used muscovite as an analogue for all the different generations of end-member illite. It is likely that this reaction is driven by a low Gibbs Free Energy, given the small differences between such mica-type minerals, and therefore that it should proceed at a very slow rate. Although this interpretation for the two-step kinetic model of Velde and Vasseur (1992) is only speculative, it raises a question concerning the nature of the source minerals involved in the illitization reaction.

The effect of organic matter maturation on the illitization rate in shales is illustrated in Fig. 3. In the absence of muscovite/illite precipitation, and with initial coexistence of K-feldspar and montmorillonite, the release of carbonic and acetic acid into the pore water increases the scale of the $|\Delta G|_{reaction}$ for muscovite/illite growth, or, in other words, the degree of saturation of the final solution with respect to muscovite/illite. This is due to the occurrence of kaolinite in the paragenesis controlling the fluid composition (see Fig. 2). In the case of shales, this also suggests that the maturation of organic matter

promotes the illitization of smectites by increasing the growth rate of the end-member illite or by helping to overcome the energy barrier of the nucleation steps.

Natural shales and sandstones are defined essentially by their grain size, which generally reflects different mineralogical compositions. Thus, the differences observed in clay diagenesis between shales and sandstones are indicative of the composition of the clay fraction. A 'sandstone-type' behaviour is expected in shales where clays consist of kaolinite, and a 'shale-type' behaviour is expected in sandstones containing smectites.

SHALE/SANDSTONE INTERACTIONS

Many authors have advanced the hypothesis that CO_2 and organic complexes released from source rocks have a major influence on mineral diagenesis in adjacent sandstones. As pointed out by Bjørlykke (1984), Giles and Marshall (1986), Bjørlykke and Aagaard (1992) and Barth and Bjørlykke (1993), such an effect implies that organic protons and ligands are not neutralized by mineral reactions before the migration of the relevant aqueous species.

Transfer of acid species

The calculations presented in the first part of this study show that when CO_2 and acetic acid are released into a mineral matrix containing hydrolysable phases, the mineral reactions are able to neutralize the acid species. Thus, when modelling the reaction at 120°C between an organic matter-free sandstone and a fluid previously equilibrated with an organic matter-bearing shale (one flushing cycle), the aqueous species of organic origin generated in the shale has little or no effect on diagenesis in the host sandstone. This is probably characteristic of most situations in shale/sandstone sequences. As a matter of fact, it is difficult to imagine convection circulation through shales and—except for coals, where the organic fraction may dominate the mineral fraction—shales and source rocks generally contain sufficient amounts of detrital feldspar to neutralize organic protons. As an example, Bjørlykke and Aagaard (1992) have suggested this effect could explain why the Upper Jurassic Sandstones of the North Sea, which are interbedded with source rocks, show very little evidence of feldspar leaching and kaolinite precipitation at the contact with the source rocks. In the case of coals, Gaupp et al. (1993) and Platt (1993) have proposed that the kaolinitization of feldspar in adjacent sandstones might result from the supply of coal-derived acid material to the sandstones. When acid species of organic origin are free to leave the source rocks (insufficient hydrolysable minerals in the source rock, or transfer by a hydrocarbon phase), the diagenetic reactions in the host sandstones can be accounted for

by the simulations of the organic material-bearing sandstones. In the light of the discussion about the illitization reaction in sandstones, it can be stated that feldspar hydrolysis produces kaolinite—not illite—because the critical $|\Delta G|_{reaction}$ for illite growth is not reached if the pore water is undersaturated or equilibrated with respect to K-feldspar. The illitization of kaolinite reported by Gaupp et al. (1993) and Platt (1993) can be more realistically attributed to an influx of brines from the overlying Zechstein formation (see Lanson et al., 1996 for further evidence), or any other posterior mechanism increasing the pH of the organic-derived fluid (dissolution of distant carbonates by aqueous diffusion of protons?) and causing pore water to reach the critical oversaturation state for illite growth.

Effect of ligands on fluid chemistry in source rocks

The effect of organic diagenesis on fluid chemistry can be examined using simulations of shale diagenesis. We found that the formation of organic complexes in solution increases the solubility of Mg, and, to a lesser extent, Ca, whereas Al- and Fe-acetates were present only as traces. As an example, the speciation of Ca, Mg and acetate in the shale fluid at 120°C is shown in Fig. 6 (light-coloured bars). Although the CH_3COO^- ion dominates the acetate species in solution (> 90%), the acetate complexes account for 55% of the dissolved Mg and 22% of the dissolved Ca. The degree of complexation of cations depends both on pH and on the amount of released organic acid. Thus,
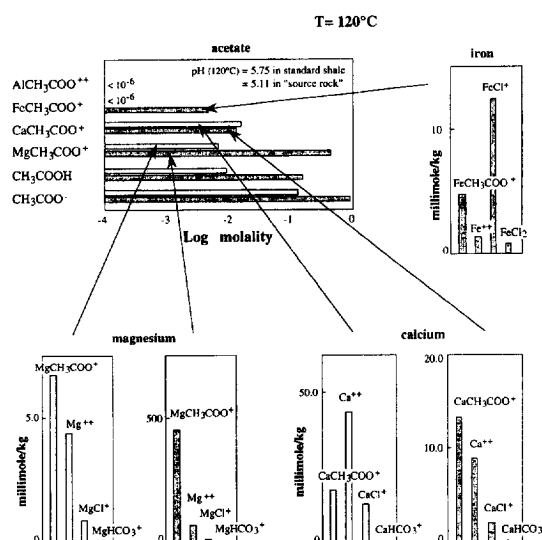

Fig. 6. Speciation of the shale fluid at 120°C before the decomposition of aqueous acetate species. The light-coloured bars correspond to a 'standard' shale according to Table 2 ($\approx 0.18\%$ TOC in rock). The dark-coloured bars correspond to a shale rich in organic matter ($\approx 1.8\%$ TOC in rock and $fO2(g) = 10^{-54}$ bars).

the complexation of cations may become an essential parameter for controlling fluid chemistry in natural source rocks, due to the amount of CO_2 and organic acid generated by the thermal degradation of kerogen, since this amount can be much higher than that expected here. To illustrate the effect of organic acids on fluid chemistry in source rocks, we simulated shale diagenesis at 120°C by increasing the amount of CO_2 and acetic acid by one order of magnitude. Assuming hydrocarbon phase generation at 120°C, we also fixed the fugacity of $O_2(g)$ at 10^{-54} bars. Under these conditions, fugacity for the aqueous phases of $CH_4(g)$, $CO_2(g)$ and $H_2S(g)$ at the end of reaction was 400 bars, 2.5 bars, and 0.4 bars, respectively. The partial pressures of these components are consistent with the composition of a hydrocarbon phase. Compared with the preceding diagenesis, the secondary paragenesis is characterized by the occurrence of traces of pyrite, a carbonate fraction making up 3% of the rock, and conversion of nontronite to daphnite (allowing for a slight oversaturation of annite and minnesotaite). Figure 6 shows the speciation of the aqueous phase (dark-coloured bars) with significant changes in the solution chemistry, especially for Mg whose concentration approaches that of Na.

Stability of ligands in shales and sandstones

Taken alone, the complexation of cations by organic anions does not significantly alter the mineral matrix in shales or sandstones given the low water/ rock ratios used in this study (W/R <0.1). However, the decarboxylation of organometallic complexes produces carbonates with associated cations. Kharaka *et al.* (1983), Palmer and Drummond (1986) and Bell *et al.* (1994) have shown that the decomposition of acetate depends on temperature, fluid chemistry and the nature of the mineral surfaces exposed to pore waters, and, more particularly, the rate of acetate decomposition is increased by the reduction of Fe^{3+} to Fe^{2+} on available surfaces. From this experimental evidence, it appears that organic complexes are less stable in oxidizing conditions (i.e. in sandstone containing Fe^{3+}-bearing phases) than under reducing conditions (i.e. in source rock where $fO_2(g)$ is buffered at low values).

Transfer of organometallic complexes from shale to sandstone and carbonate cementation in sandstone

An attempt was made to determine the effects of a mass transfer mechanism caused by the production and decomposition of organic acids that are spatially disconnected due to the Eh gradient. The production of metastable organometallic complexes in shales rich in organic matter is assumed to be followed by their transfer and decomposition (carbonate precipitation) in adjacent sandstones where Fe^{3+}-bearing phases act

as catalysts. For the illitization reaction, shale and sandstone may be differentiated not only by their grain size but also by their chemical composition (Eh conditions). As a first approach, we assumed advective transfer of aqueous species by replacing the sandstone fluid by the shale fluid previously equilibrated at 120°C. In this simulation, the amount of precipitated carbonate for one flushing cycle is negligible. Since convective fluid flow through shales is hardly conceivable, the diffusion of aqueous species was adopted as an alternative migration mechanism. Drummond and Palmer (1986) and Barth and Nielsen (1993) reported values of activation energy as high as 250–275 kJ mol^{-1} for acetate decarboxylation. Compared with the low activation energy values obtained for the diffusion of aqueous organic species (13.8 kJ mol^{-1} at temperatures above 100°C; Oelkers, 1991), the probability that acetate decomposition is faster than diffusion increases with temperature. This suggests that carbonate cementation may occur at high temperatures within the source rock. However, within the range of the moderate temperatures considered here (<150°C), Fe^{3+}-bearing minerals are thought to have an important catalytic effect on acetate decomposition (Bell *et al.*, 1994). Accurate modelling of such a process should incorporate the kinetics of organic species formation in shales as well as the rate of decarboxylation in sandstones, using mass transfer equations versus time, space and temperature. The significance of diffusion in diagenesis can be more easily measured by the steady concentration gradient observed in the acetate complexes occurring in shales and sandstones. The amount of Mg- or Ca-acetate transferred from shales to sandstones during one million a at 100°C is calculated here by application of Fick's law in a steady flow regime. Taking porosity as equal to 22%, the diffusion coefficient of acetate as 4.63×10^{-5} cm^2 s^{-1} (Oelkers, 1991) and the acetate gradient as 10^{-6} molal cm^{-1}, the resulting acetate flux at the shale/sandstone interface is 3.2×10^{-3} mole m$^{2-1}$ a^{-1}. Assuming each mole of acetate complex produces one mole of carbonate in the sandstone, the corresponding filling of the pore space is shown in Fig. 7 together with the thickness of a sandstone layer containing 10% authigenic carbonate by volume. The thickness of carbonate cementation produced during one million a amounts to about 1.2 m. It should be noted that this amount of such authigenic carbonate depends on the amount of organic C produced in the adjacent source rock. Although this model is oversimplified and the acetate gradient is chosen arbitrarily, Fig. 7 illustrates, nevertheless, the importance of the diffusion of aqueous species in heterogeneous systems. The diffusion of aqueous species has also been reported by Berger *et al.* (1992) to explain mass transfers between the wall–rock and fractures of a hydrothermally altered granite. It is noteworthy that chemical gradients can produce a mass transfer provided that the boundary conditions
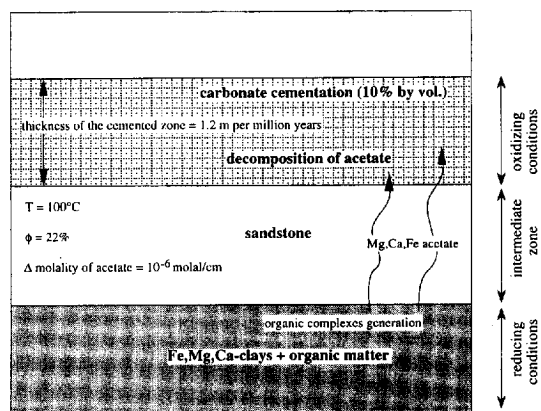
Fig. 7. Reaction pathway for the diffusion of organic complexes from shales to sandstones and decomposition of these organic complexes in sandstones.
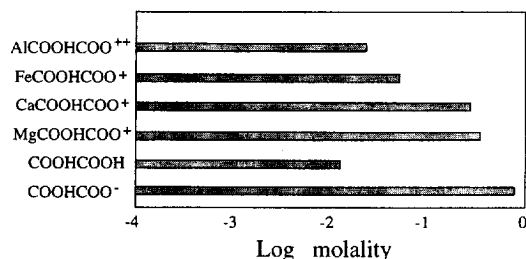

Fig. 8. Speciation of the aqueous oxalate species in a shale rich in organic material, using oxalic acid to model the formation of organic acid.

are maintained. In the case of organic acid migration, acetate decarboxylation can also lead to CH_4 production. If this reducing species is not removed from sandstones, the O_2 fugacity in pore waters and the decomposition rate of acetate will decrease with time regardless of the chemical potential for transfer. Fluid flow through sandstones appears here as the most appropriate mechanism for maintaining the boundary conditions. However, even if such a process is physically possible, the presence of diagenetic Ca–Mg–Fe-carbonates at the sandstone/shale contact zone has only been described in a few studies (Moncure et al., 1984; Galy et al., 1993). Deep carbonate cementation in sandstones is rarely of organic origin, a conclusion based on the fact that the isotopic signature of C is generally not of organic origin. If the pore fluid of the host rock contains aqueous carbonate of mineral origin, which is usually the case, the isotopic signature of the carbonate cement could be dominated by mineral C, even though Ca, Mg and Fe may be transported by organic complexes.

Transfer of aluminum

Transfer of Al by means of organometallic complexes has been proposed by some authors as a mechanism likely to induce precipitation of cements distant from the corresponding source mineral dissolution sites (MacGowan and Surdam, 1988; Surdam et al., 1989a, 1989b; Fein et al., 1994). For the present calculations, we only took into account acetate complexes. Results show that the complexation of Al as acetate is negligible when Mg, Ca and Fe compete with Al and when pore water with a near-neutral pH is buffered by the mineral matrix. According to Harrison and Thyne (1992) and Fein et al. (1994), oxalic acid appears to be a more efficient ligand for Al in the 4–6 pH range. Using the association constant of

metal–oxalate complexes proposed by Harrison and Thyne (1992), we modelled the diagenesis at 120°C in a shale (source rock) rich in organic matter with oxalate as the organic acid. The speciation of equilibrated pore water is shown in Fig. 8. It can be seen from this figure that even though oxalate increases significantly, the solubility of Al, compared with that of acetate, Mg-, Ca-, or Fe-oxalates are still dominant in the organic complexes in solution. Note that this modelled situation corresponds to an extreme case. In particular, the precipitation of Ca or Fe-oxalate minerals (not considered here) can buffer the oxalate contents in the fluid. From these simulations, it appears that conditions such as low pH, absence of Mg or Ca, Fe, as well as predominance of oxalates over other organic anions must combine additively to complex and transport Al selectively so as to form aluminous phases (kaolinite). Such a process has been investigated experimentally by Small (1993). However, this set of conditions indicates that subsequent Al transfer (in the form of organic complexes) is of minor importance in natural environments.

CONCLUSIONS

From similarities or discrepancies between the numerical results of thermo-kinetic modelling and field data, we identify two mechanisms that control the illitization reaction observed in clastic sediments, depending on the nature of the clay. We also evaluate the effect of organic matter maturation on diagenesis in sandstone/shale sequences.

(1) Kaolinite conversion to end-member illite involves a high energy barrier (> 2 kcal mol^{-1}), which is not overcome when the pore water equilibrates with the mineral matrix in closed systems. To overcome this barrier, the fluid must be oversaturated with respect to K-feldspar. The metastability of the kaolinite–quartz–K-feldspar assemblage is not attributed to a lack of time but to the absence of appropriate conditions. An external source of K or a pH increase in an open system is a necessary condition for this

reaction. No particular evidence can be found of the effect of organic diagenesis on this reaction.

(2) The slow but systematic conversion of smectite to illite observed in shales indicates that smectite precursors weaken the barrier to illite nucleation and growth. The time–temperature dependence of this reaction reported in the literature suggests that the hydrolysis of K-feldspar is the source of K during most of the reaction. Organic matter maturation may increase the reaction rate by increasing the Gibbs Free Energy of illite growth.

(3) As the mineral matrix tends to buffer pore water at near-neutral pH values, except for extreme cases such as coals, the migration of shale-derived water-soluble organic species to sandstones does not seem to be capable of initiating subsequent acid-base reactions in the host sandstone. On the other hand, the diffusion of Mg and Ca in the form of organic complexes and the decomposition of these complexes under oxidizing conditions in sandstones may lead to carbonate cementation in the adjacent sandstones. An oxidizing fluid flow through sandstones appears here as a factor maintaining the boundary conditions (Eh gradient) rather favouring the transfer mechanism for Ca^{++}, Mg^{++}, Fe^{++} and CO_3^-.

Editorial Handling: Dr B. R. T. Simoneit.

REFERENCES

Andresen B., Thronsen T., Barth T. and Bolstad J. (1994) Thermal generation of carbon dioxide and organic acids from different source rocks. *Organic Geochem.* 21, 1229–1242.

Barth T. (1991) Organic acids and inorganic ions in waters from petroleum reservoirs, Norwegian continental shelf: a multivariate statistical analysis and comparison with American reservoir formation waters. *Appl. Geochem.* 6, 1–15.

Barth T. and Bjørlykke K. (1993) Organic acids from source rock maturation: generation potential of transport mechanisms and relevance for mineral diagenesis. *Appl. Geochem.* 8, 325–337.

Barth T. and Nielsen S. B. (1993) Estimating kinetic parameters for generation of petroleum and single components from hydrous pyrolysis of source rocks. *Energy Fuels* 7, 100–110.

Bell J. L. S., Palmer D. A., Barnes H. L. and Barnes H. L. (1994) Thermal decomposition of acetate: III. Catalysis by mineral surfaces. *Geochim. Cosmochim. Acta* 58, 4155–4177.

Ben Baccar M., Fritz B. and Brévart O. (1993) Geochemical modelling of late diagenetic processes in the Brent Sandstone, Alwyn South area (East Shetland Basin, North Sea). 1. Estimation of the circulated fluids composition. *Chem. Geol.* 109, 135–147.

Berger, G. (1995) The dissolution rate of sanidine at near neutral pH as a function of silica activity at 100, 200, and 300°C. In *Water–Rock-Interaction* (eds Y. K Kharaka and O. Chudaev), Balkema, Rotterdam, 141–144.

Berger G., Turpault M. P. and Meunier A. (1992) Dissolution–precipitation processes induced by hot water

in a fractured granite. Part 2: modelling of water–rock interaction. *Eur. J. Mineral.* 4, 1477–1488.

Berger G., Cadoré E., Schott J. and Dove P. M. (1994) Dissolution rate of quartz in Pb and Na electrolyte solutions between 25 and 300°C. Effect of the nature of the surface complexes and reaction affinity. *Geochim. Cosmochim. Acta* 58, 541–551.

Bjørkum P. A. and Gjelsvik N. (1988) An isochemical model for formation of authigenic kaolinite, K-feldspar and illite in sediments. *J. Sedim. Petrol.* 57, 166–183.

Bjørlykke K. (1984) Formation of secondary porosity: how important is it? *AAPG Mem.* 37, 227–286.

Bjørlykke K. and Aagaard P. (1992) Clay minerals in North Sea sandstones. In Origin, Diagenesis, and Petrophysics of Clay Minerals in Sandstones. *SEPM Special Publication* 47, 65–80.

Burch T. E., Nagy K. L. and Lasaga A. C. (1993) Free energy dependence of albite dissolution kinetics at 80°C and pH 8.8. *Chem. Geol.* 105, 137–162.

Busenberg E. and Clemency C. V. (1976) The dissolution kinetics of feldspars at 25°C and 1 atm CO_2 partial pressure. *Geochim. Cosmochim. Acta* 40, 41–51.

Carroll S. E. and Walther J. V. (1990) Kaolinite dissolution at 25°, 60° and 80°C. *Am. J. Sci.* 290, 797–810.

Chermack J. A. and Rimstidt J. D. (1990) The hydrothermal transformation rate of kaolinite to muscovite/illite. *Geochim. Cosmochim. Acta* 54, 2979–2990.

Dove P. M. and Crerar D. A. (1990) Kinetics of quartz dissolution in electrolyte solutions using a hydrothermal mixed-flow reactor. *Geochim. Cosmochim. Acta* 54, 955–969.

Drummond S. A. and Palmer D. A. (1986) Thermal decarboxylation of acetate. Part II. Boundary conditions for the role of acetate in the primary migration of natural gas and the transportation of metals in hydrothermal systems. *Geochim. Cosmochim. Acta* 50, 825–833.

Eberl D. D. (1993) Three zones for illite formation during burial diagenesis and metamorphism. *Clays and Clay Miner.* 41, 26–37.

Egeberg P. K. and Aagaard P. (1989) Origin and evolution of formation waters from oil fields on the Norwegian shelf. *Appl. Geochem.* 4, 131–142.

Ehrenberg S. N. (1991) Kaolinized, potassium-leached zones at the contacts of the Garn Formation, Haltenbanken, mid-Norwegian continental shelf. *Mar. Petrol. Geol.* 8, 250–269.

Ehrenberg S. N., Aagaard P., Wilson M. J., Frazer A. R. and Duthie D. M. L. (1993) Depth-dependent transformation of kaolinite to dickite in sandstones of the Norwegian continental shelf. *Clay Miner.* 28, 325–352.

Fein J. B., Yane L. and Handa T. (1994) The effect of aqueous complexation on the decarboxylation rate of oxalate. *Geochim. Cosmochim. Acta* 58, 3975–3981.

Galy A., Coleman M. L. and Evans J. (1993) Derived organic carbon in Mam Tor (Derbyshire—England). Relation between black shales and carbonate cement in turbidite. EUG-7, Strasbourg, France. Terra Abstract, p. 638.

Gaupp R., Matter A., Platt J., Ramseyer K. and Walzebuck J. (1993) Diagenesis and fluid evolution of deeply buried Permian (Rotliegend) gas reservoirs, Northwest Germany. *AAPG Bull.* 77, 111–1128.

Giles M. R. and Marshall J. D. (1986) Constraints on the development of a secondary porosity in the subsurface: re-evaluation of processes. *Mar. Petrol. Geol.* 3, 243–255.

Harrison W. J. and Thyne G. D. (1992) Prediction of diagenetic reations in the presence of organic acids. *Geochim. Cosmochim. Acta* 56, 565–586.

Helgeson H. C. (1969) Thermodynamics of hydrothermal systems at elevated temperatures and pressures. *Am. J. Sci.* 267, 729–804.

Helgeson H. C., Murphy W. M. and Aagaard P. (1984) Thermodynamic and kinetic constraints on reaction rates

among minerals and aqueous solutions. II. Rate constants, effective surface area, and the hydrolysis of feldspar. *Geochim. Cosmochim. Acta* **48**, 2405–2432.

Hellmann R. (1994) The albite–water system: Part I. The kinetics of dissolution as a function of pH at 100, 200, and 300°C. *Geochim. Cosmochim. Acta* **58**, 595–611.

Hower J., Eslinger E. V., Hower M. and Perry E. A. (1976) Mechanism of burial metamorphism of argillaceous sediments. I. Mineralogical and chemical evidence. *Bull. geol. Soc. Am.* **87**, 725–737.

Kharaka Y. K., Carothers W. and Rosenbauer R. J. (1983) Thermal decarboxylation of acetic acid: implications for origin of natural gas. *Geochim. Cosmochim. Acta* **47**, 397–402.

Kharaka Y. K., Hull R. W. and Carothers W. (1985) Water–rock interaction in sedimentary basins. In *Relationship of Organic Matter and Mineral Diagenesis* (eds D. L. Gautier, Y. K. Kharaka and R. C. Surdam) *Soc. Econ. Paleont. Mineral.* **17**, 79–174.

Lanson B. and Champion D. (1991) The I/S to illite reaction in the late stage diagenesis. *Am. J. Sci.* **291**, 473–506.

Lanson B., Beaufort D., Berger G., Petit S. and Lacharpagne, J. C. (1996) Illitization of diagenetic kaolinite-to-dickite conversion series: The Lower Permian Rotliegend sandstone reservoir, offshore of The Netherlands. *J. Sedim. Res.* **66**, 501–518.

Lin F. and Clemency C. V. (1981) The kinetics of dissolution of muscovites at 25°C and 1 atm CO_2 partial pressure. *Geochim. Cosmochim. Acta* **45**, 571–576.

MacGowan D. B. and Surdam R. C. (1988) Difunctional carboxylic acid anions in oilfield waters. *Org. Geochem.* **12**(3), 245–259.

Matthews J., Velde B. and Johansen H. (1994) Significance of K–Ar ages of authigenic illite clay minerals in some sandstones and shales from the North Sea. *Clay Minerals* **29**, 379–390.

Moncure G. K., Lahann R. W. and Siebert R. M. (1984) Origin of secondary porosity and cement distribution in a sandstone/shale sequence from the Frio Formation (Oligocene). In *Clastic Diagenesis* (eds D. A. MacDonald and R. C. Surdam) *AAPG Mem.* **37**, Tulsa, Oklahoma pp. 151–162.

Nagy K. L., Blum A. E. and Lasaga A. C. (1991) Dissolution and precipitation kinetics of kaolinite at 80°C and pH 3: The dependence on solution saturation state. *Am. J. Sci.* **291**, 649–686.

Nonaka A. (1984) Surface area estimation from the adsorption isotherm gradient at the linear portion by benzene and toluene vapors on mica and aluminum foil samples. *J. Colloid. Interface Sci.* **99**, 335–340.

Oelkers E. H. (1991) Calculation of diffusion coefficients for aqueous organic species at temperatures from 0 to 350°C. *Geochim. Cosmochim. Acta* **55**, 3515–3529.

Oelkers E. H., Schott J. and Devidal J. L. (1994) The effect of aluminum, pH, and chemical affinity on the rates of aluminosilicate dissolution reactions. *Geochim. Cosmochim. Acta* **58**, 2011–2024.

Palmer D. A. and Drummond S. A. (1986) Thermal decarboxylation of acetate. Part I. The kinetics and mechanism of reaction in aqueous solution. *Geochim. Cosmochim. Acta* **50**, 813–823.

Platt J. D. (1993) Controls on clay mineral distribution and chemistry in the early Permian Rotliegend of Germany. *Clay Miner.* **28**, 393–416.

Pye K. and Krinsley D. H. (1986) Diagenetic carbonate and evaporite minerals in Rotlingend aeolian sandstones of the southern North Sea: their nature and relationship to secondary porosity development. *Clay Miner.* **21**, 443–457.

Rimstidt J. D. and Barnes H. L. (1980) The kinetics of silica–water reactions. *Geochim. Cosmochim. Acta* **44**, 1683–1699.

Rossel N. C. (1982) Clay mineral diagenesis in Rotliegend aeolian sandstones of the Southern North Sea. *Clay Mineral.* **17**, 69–77.

Small J. S. (1993) Experimental determination of the rates of precipitation of authigenic illite and kaolinite in the presence of aqueous oxalate and comparison to the K/Ar ages of authigenic illite in reservoir sandstones. *Clays and Clay Miner.* **41**(2), 191–208.

Srodon J., Morgan D. J., Eslinger E. V., Eberl D. D. and Karlinger M. R. (1986) Chemistry of illite/smectite and end member illite. *Clays and Clay Miner.* **34**(4), 368–378.

Surdam R. C., MacGowan D. B. and Dunn T. L. (1989) Diagenetic pathways of sandstone and shale sequences. *Contrib. Geol.* **27**, 21–31.

Surdam R. C., Crossey L. J., Hagen E. S. and Heasler H. P. (1989) Organic–inorganic interactions and sandstone diagenesis. *AAPG Bull.* **73**, 1–23.

Velde B. and Vasseur G. (1992) Estimation of the diagenetic smectite to illite transformation in time–temperature space. *Am. Miner.* **77**, 967–976.

White A. and Peterson M. L. Role of reactive surface area characterization in geochemical kinetic models. In *Chemical modeling of Aqueous Systems II* (ed. D. C. Melchior and R. L. Basset). *ACS Symposium Series* **416**, 461–475.

Wolery T. J. (1983) EQ3NR, a computer program for geochemical aqueous speciation solubility calculations: user's guide and documentation. Lawrence Livermore National Laboratory, Livermore, CA, UCRL-53414.

Wolery T. J. and Daveler S. A. (1990) EQ6, a computer program for reaction path modeling of aqueous geochemical systems: user's guide and documentation. Lawrence Livermore National Laboratory, Livermore, CA, UCRL-reports.